

Supporting Information

Nanophotonic sialidase immunoassay for bacterial vaginosis diagnosis

Cynthia Rodríguez-Nava^{a,b}, Karen Cortés-Sarabia^b, Mariana D. Avila-Huerta^a, Edwin J. Ortiz-Riaño^a, Ana K. Estrada-Moreno^b, Luz del C. Alarcón-Romero^b, Olga Mata-Ruíz^c, Yolanda Medina-Flores^c, Amalia Vences-Velázquez^b, Eden Morales-Narváez^{a,}.*

^a Biophotonic Nanosensors Laboratory, Centro de Investigaciones en Óptica A. C., León 37150, Guanajuato, Mexico

^b Facultad de Ciencias Químico Biológicas, Universidad Autónoma de Guerrero, Chilpancingo 39070, Guerrero, Mexico

^c Laboratorio de Anticuerpos Monoclonales, Instituto de Diagnóstico y Referencia Epidemiológicos “Dr. Manuel Martínez Báez”, Francisco de P. Miranda 177, Lomas de Plateros 01480, Ciudad de México, Mexico

Table of Contents

Figure S1. Optimization of nanoBV in terms of antibody concentration.

Figure S2. Optimization of nanoBV in terms of GO concentration.

Figure S3. Calibration curves resulting from data obtained at minute 120 of the studied nanoimmunoassay.

Figure S4. Calibration curves resulting from data obtained at minute 120 of the studied nanoimmunoassay.

Figure S5. Calibration curves of the optimized SLD nanoimmunosensing platform operating at different times.

Figure S6. Analytical performance of an indirect ELISA targeting SLD.

Figure S7. Calibrations plots (left) and the resulting SLD levels across different assays according to the clinical samples previously classified via Amsel criteria (right).

Figure S8. Calibrations plots (left) and the resulting SLD levels across different assays according to the clinical samples previously classified via Amsel criteria (right).

Figure S9. Fluorescence quenching kinetics resulting from each vaginal swab sample analyzed in this research.

Figure S10. The estimated SLD levels corresponding to each sample, resulting from the analysis facilitated by nanoBV.

Figure S11. Pictures of the overall biosensing platform.

Table S1. Limit of detection (LOD) and determination coefficient (R^2) of nanoBV operating in different conditions.

Table S2. Evaluation of the analytical performance of nanoBV across time.

Table S3. Evaluation of the precision of nanoBV in terms of CV.

Table S4. Estimation of cost of the indirect ELISA and nanoBV.

Table S5. Technical comparison between indirect ELISA and nanoBV.

Table S6. Evaluation of the precision of nanoBV in terms of CV.

Table S7. Evaluation of the LOD of nanoBV across different assays.

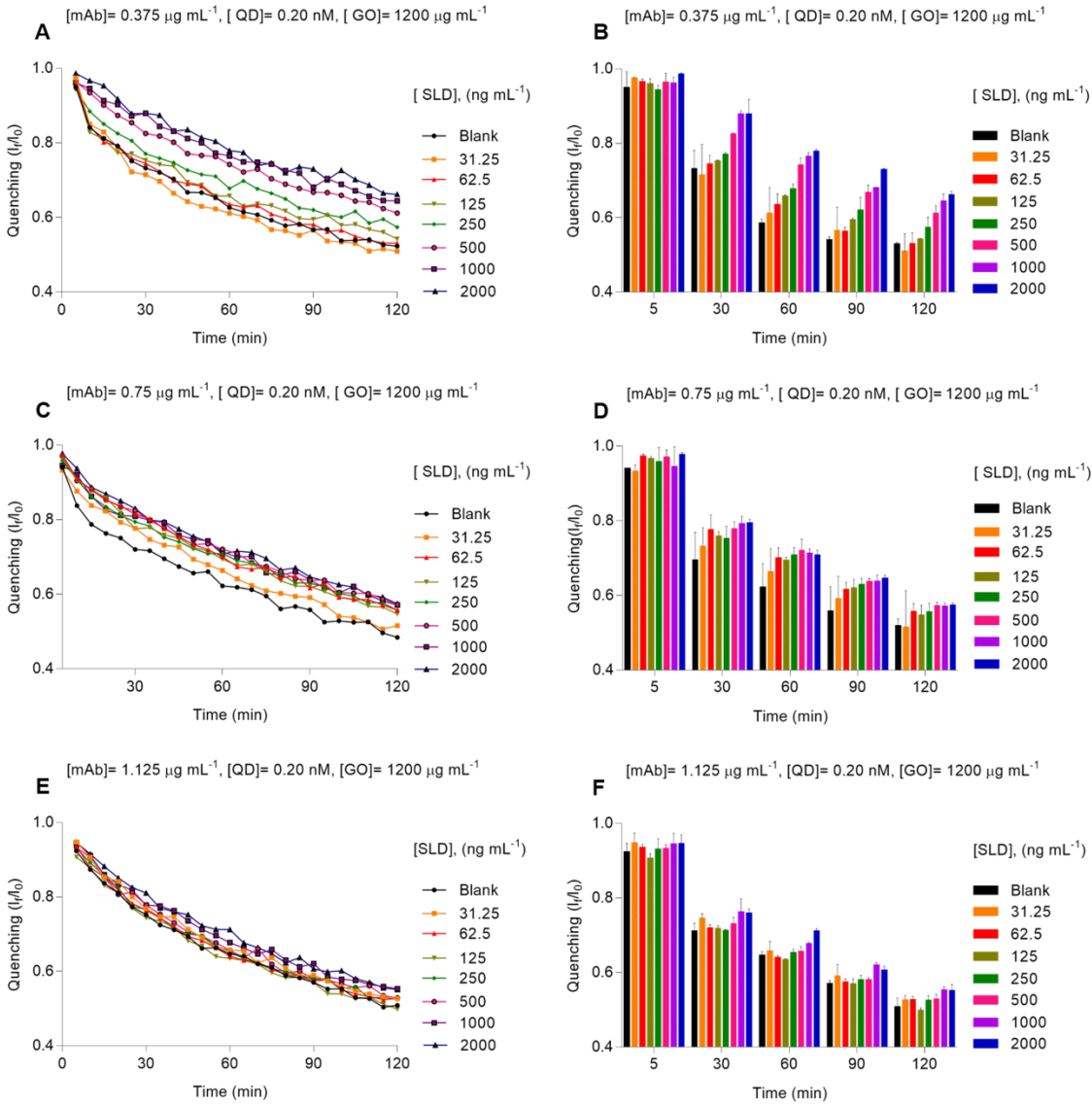


Figure S1. Optimization of nanoBV in terms of antibody concentration. A-B) Experimental evidence using mAb concentrated at $0.375 \mu\text{g mL}^{-1}$. C-D) Experimental evidence using mAb concentrated at $0.75 \mu\text{g mL}^{-1}$. E-F) Experimental evidence using mAb concentrated at $1.125 \mu\text{g mL}^{-1}$. All the plates were coating with GO concentration at $1200 \mu\text{g mL}^{-1}$. The final QD concentration was at 0.20 nM . The error bars represent the standard deviation of the three parallel experiments.

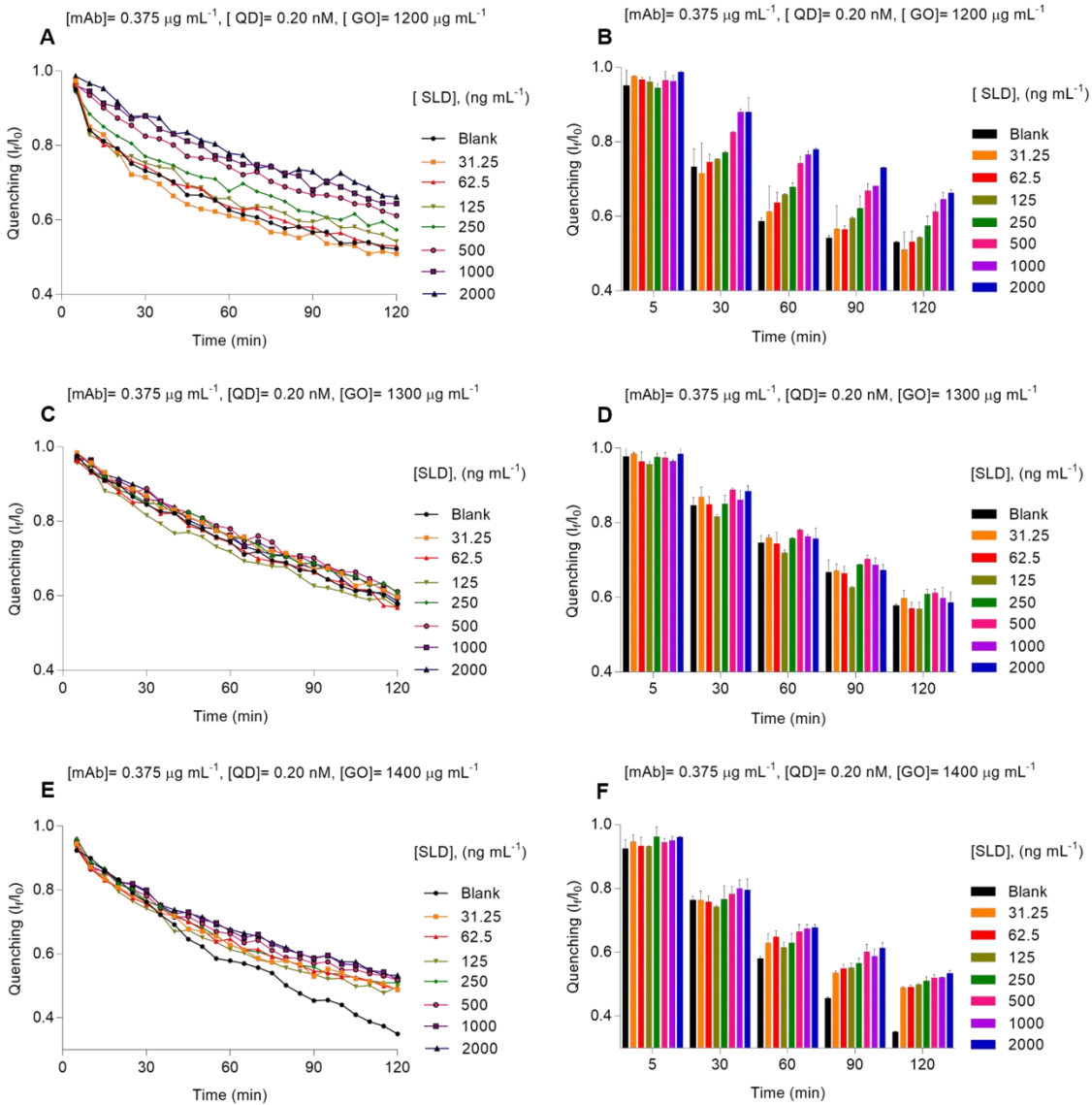


Figure S2. Optimization of nanoBV in terms of GO concentration. A-B) Experimental evidence using GO concentrated at 1200 μg mL⁻¹. C-D) Experimental evidence using GO concentrated at 1300 μg mL⁻¹. E-F) Experimental evidence using GO concentrated at 1400 μg mL⁻¹. All the experiments were performed with antibody concentration at 0.375 μg mL⁻¹. The final QD concentration was 0.20 nM. The error bars represent the standard deviation of the three parallel experiments.

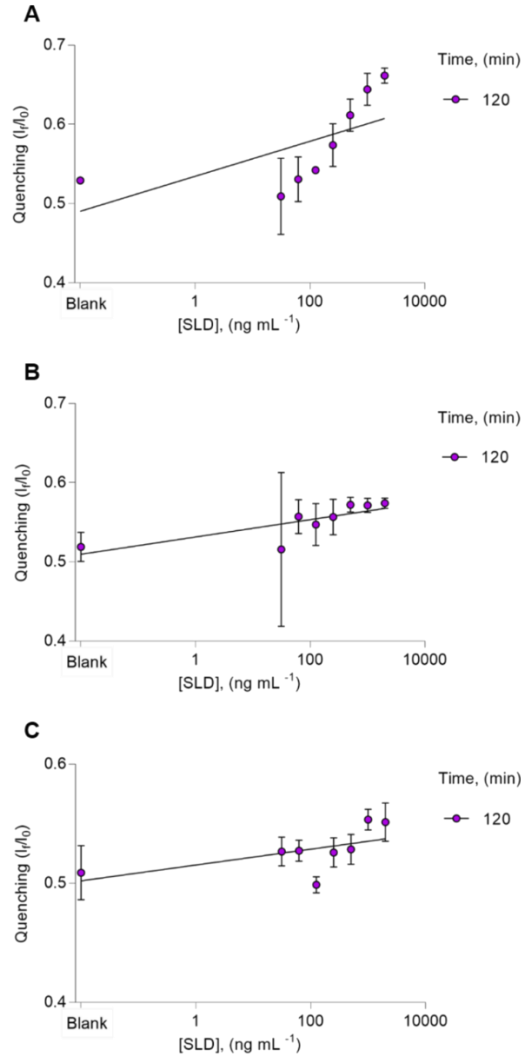


Figure S3. Calibration curves resulting from data obtained at minute 120 of nanoBV (optimization in terms of mAb concentration, see Figure S1). A) Experimental evidence using antibody concentrated at $0.375 \mu\text{g mL}^{-1}$. B) Experimental evidence using antibody concentrated at $0.75 \mu\text{g mL}^{-1}$. C) Experimental evidence using antibody concentrated at $1.125 \mu\text{g mL}^{-1}$. All the plates were coating with GO concentration at $1200 \mu\text{g mL}^{-1}$ and SLD in double dilutions at $31.25 - 2000 \text{ ng mL}^{-1}$. The final QD concentration was at 0.20 nM mL^{-1} . The error bars represent the standard deviation of the three parallel experiments.

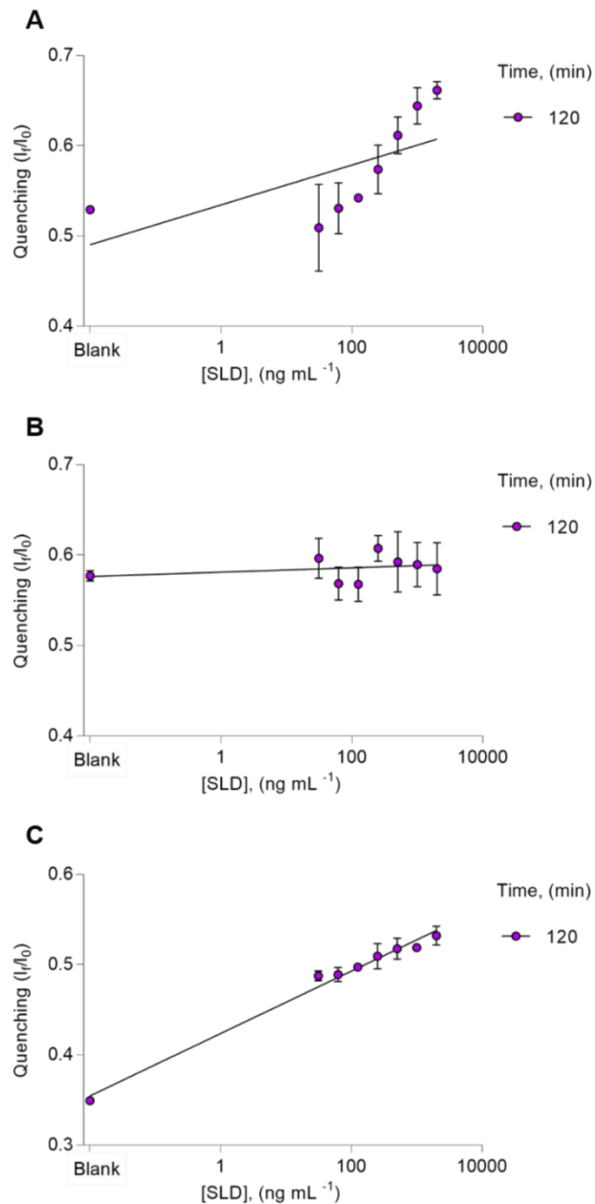


Figure S4. Calibration curves resulting from data obtained at minute 120 of nanoBV (optimization in terms of GO concentration, see Figure S2). A) Experimental evidence using GO concentrated at 1200 $\mu\text{g mL}^{-1}$. B) Experimental evidence using GO concentrated at 1300 $\mu\text{g mL}^{-1}$. C) Experimental evidence using GO concentrated at 1400 $\mu\text{g mL}^{-1}$. All the experiments were performed with antibody concentration at 0.375 $\mu\text{g mL}^{-1}$ and SLD in double dilutions at 31. 25 – 2000 ng mL^{-1} . The final QD concentration was at 0.20 nM mL^{-1} . The error bars represent the standard deviation of the three parallel experiments.

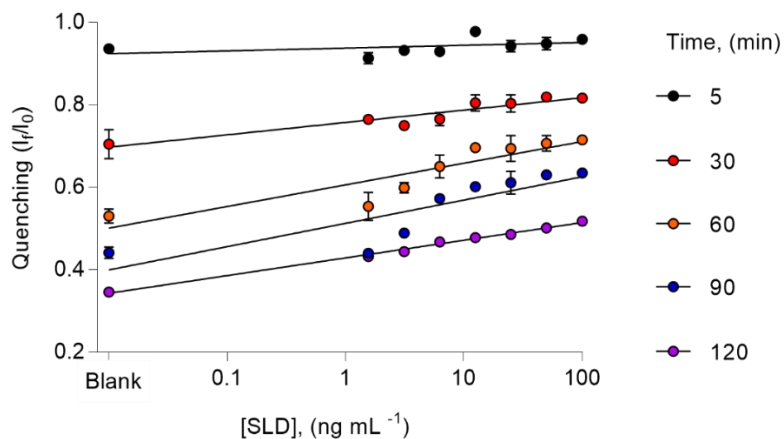


Figure S5. Calibration curves of the optimized SLD nanoimmunosensing platform operating at different times, see Figure 2.

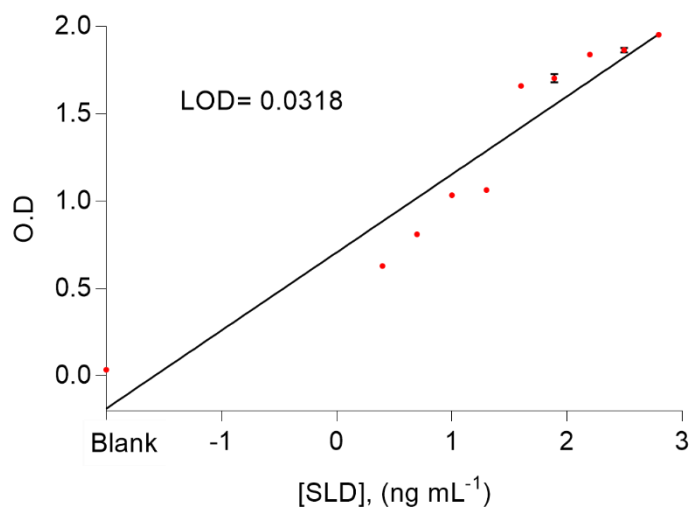


Figure S6. Analytical performance of an indirect ELISA targeting SLD. mAb was used as a primary antibody, whereas an anti-H + L antibody was used as a secondary antibody. The error bars represent the standard deviation of three parallel experiments.

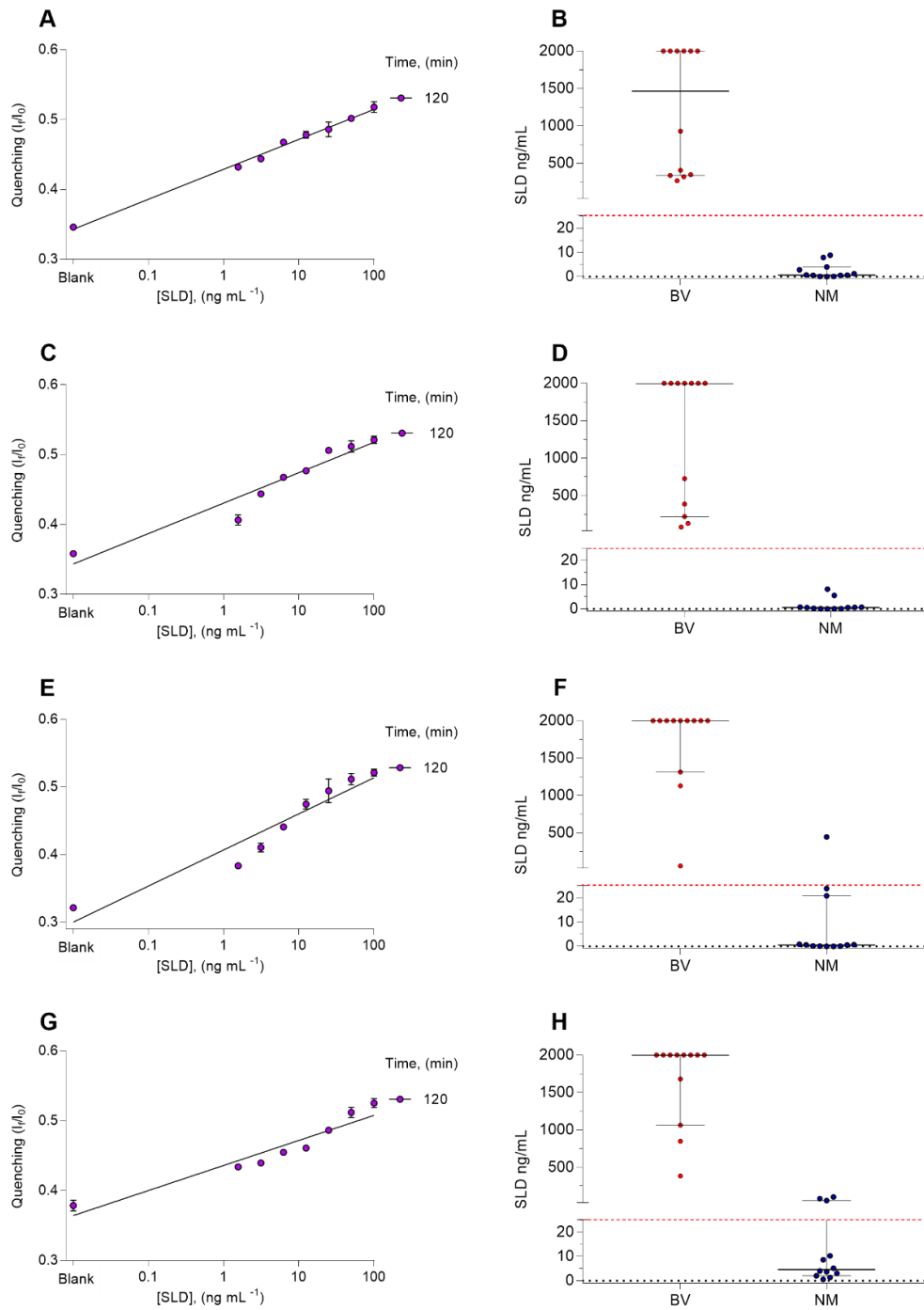


Figure S7. Calibrations plots (left) and the resulting SLD levels across different assays according to the clinical samples previously classified via Amsel criteria (right). A-B) Assay 1. C-D. Assay 2. E-F) Assay 3. G-H) Assay 4.

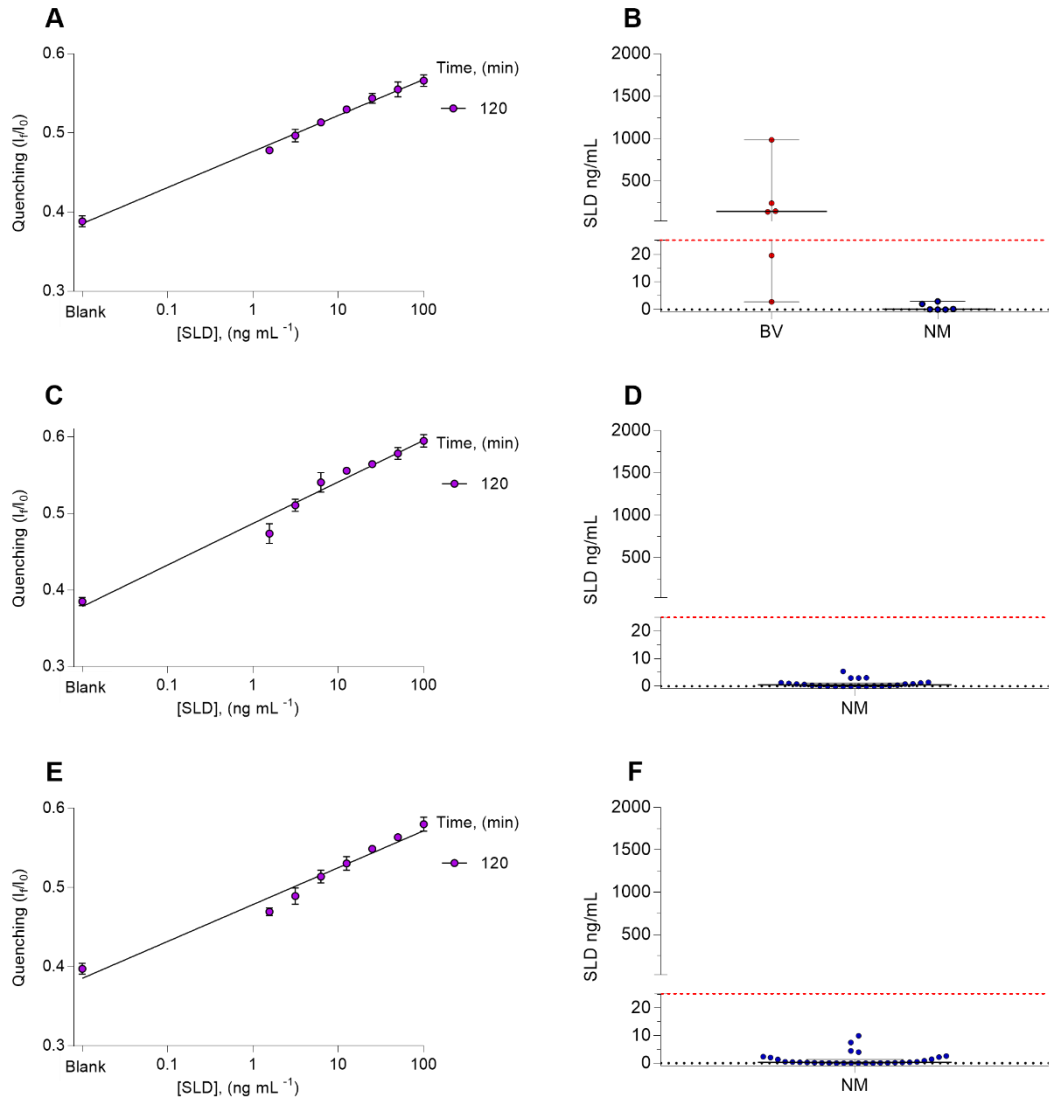


Figure S8. Calibrations plots (left) and the resulting SLD levels across different assays according to the clinical samples previously classified via Amsel criteria (right). A-B) Assay 5. C-D) Assay 6. E-F) Assay 7.

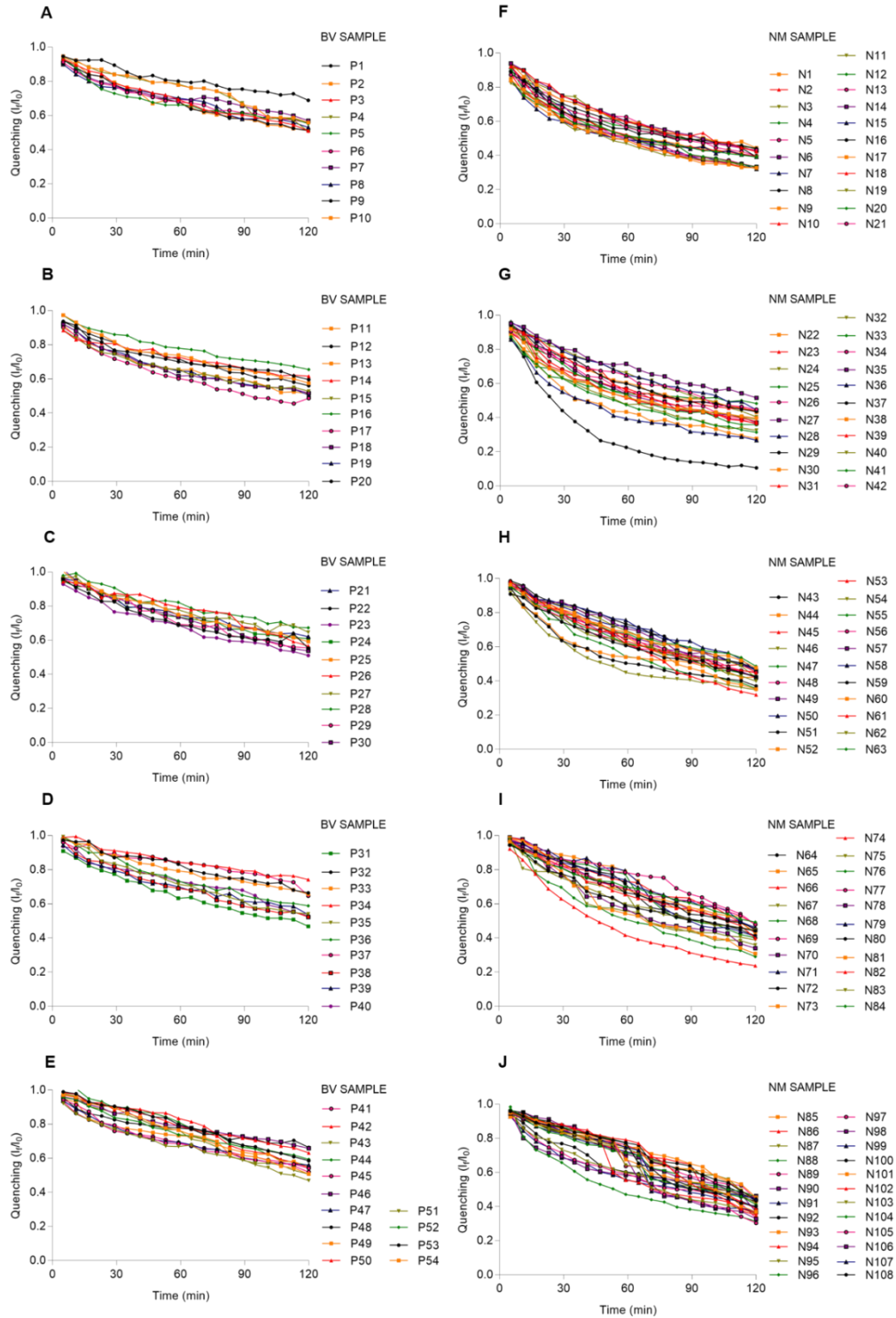


Figure S9. Fluorescence quenching kinetics resulting from each vaginal swab sample analyzed in this research using nanoBV. A-E) Samples previously classified as BV positive via Amsel criteria. F-J) Samples previously classified as normal microbiota via Amsel criteria.

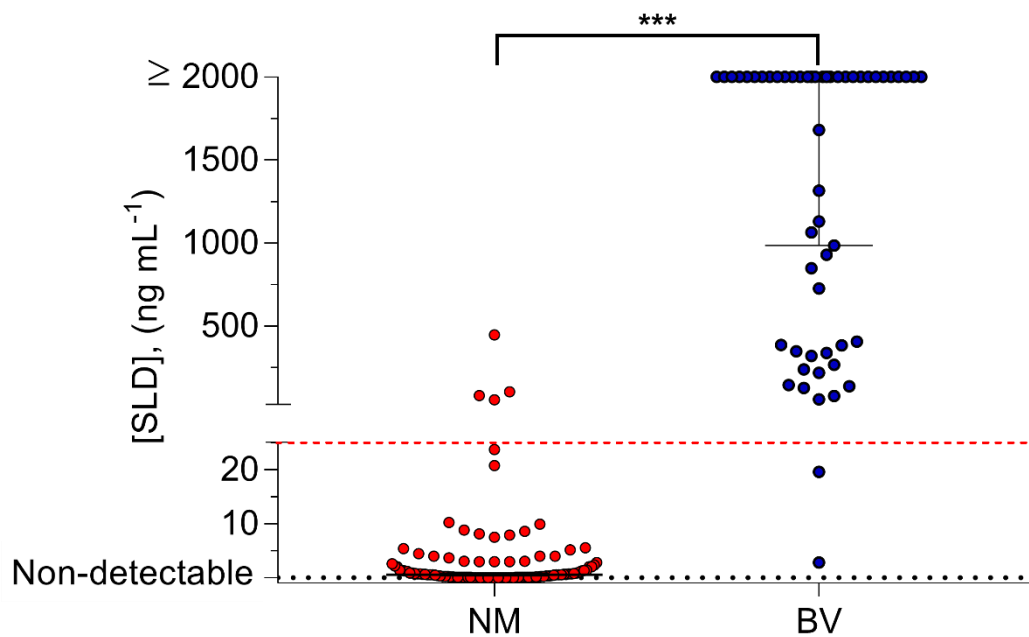


Figure S10. The estimated SLD levels corresponding to each sample, resulting from the analysis facilitated by nanoBV. The vaginal swab samples were classified in two groups according to Amsel criteria: bacterial vaginosis positive (BV, n = 54 samples) and normal microbiota (NM, n = 108 samples). The red dotted line represents the threshold (c.a. 25.194 ng mL⁻¹) employed to estimate the clinical sensitivity and specificity of nanoBV. The X² statistic test was used to obtain a *p* value accounting for <0.0001.



Figure S11. Pictures of the overall biosensing platform. Dimensions of the reader: 51.4 cm L x 41.6 cm W x 44.5 cm H. Dimensions of the microwell plate: 127.71 mm L x 85.43 mm W x 14.10 mm H.

Table S1. Limit of detection (LOD) and determination coefficient (R²) of nanoBV operating in different conditions in terms of [mAb] and [GO]. Data resulting from the calibration curves shown in Figure S3 and S4.

		LOD	R ²
		(ng mL ⁻¹)	
[GO]	[mAb]		
	0.375 μg mL ⁻¹	2.027	0.41
1200 μg mL ⁻¹	0.750 μg mL ⁻¹	8117	0.62
	1.125 μg mL ⁻¹	2183966268	0.35
[mAb]	[GO]		
	1200 μg mL ⁻¹	2.027	0.41
0.375 μg mL ⁻¹	1300 μg mL ⁻¹	192238	0.08
	1400 μg mL ⁻¹	0.0123	0.99

Table S2. Evaluation of the analytical performance of nanoBV across time. Three parallel experiments were performed in this evaluation, see Figure S5.

<i>Time (min)</i>	<i>LOD</i> <i>(ng mL⁻¹)</i>	<i>R</i> ²
5	72.25	0.185
30	64.18	0.894
60	0.35	0.805
90	0.30	0.724
120	0.012	0.994

Table S3. Evaluation of the precision of nanoBV in terms of CV. Intra-assay evaluation resulting from three parallel assays.

<i>Assay number (AN)</i>	<i>AN1</i>	<i>AN2</i>	<i>AN3</i>	<i>AN4</i>	<i>AN5</i>	<i>AN6</i>	<i>AN7</i>
<i>[SLD], ng mL⁻¹</i>	<i>CV</i>						
<i>Blank</i>	0.140 %	1.236 %	0.689 %	2.048 %	1.770 %	1.405 %	1.723 %
<i>1.56</i>	0.252 %	1.798 %	0.846 %	0.786 %	0.755 %	2.731 %	1.049 %
<i>3.13</i>	0.760 %	0.760 %	1.596 %	0.839 %	1.610 %	1.550 %	2.088 %
<i>6.25</i>	0.198 %	0.198 %	1.024 %	0.462 %	0.842 %	2.340 %	1.608 %
<i>12.5</i>	1.053 %	0.900 %	1.512 %	0.553 %	0.765 %	0.751 %	1.620 %
<i>25</i>	2.199 %	0.574 %	3.537 %	0.568 %	1.125 %	0.475 %	0.631 %
<i>50</i>	0.382 %	1.619 %	1.619 %	1.386 %	1.707 %	1.339 %	0.596 %
<i>100</i>	1.493 %	0.988 %	0.988 %	1.207 %	1.321 %	1.372 %	1.504 %

Table S4. Estimation of cost of the indirect ELISA and the nanoimmunosensing system targeting SLD.

INDIRECT ELISA		nanoBV	
Reagent	Cost per well (USD)	Reagent	Cost per well (USD)
Microwell	0.046	Plate	0.04
Carbonate buffer	9.91x10 ⁻⁰⁵	Graphene oxide	0.004
Blocking buffer	0.0016	Immunobuffer	2.6x10 ⁻⁰⁵
mAba	0.029	mAba	0.0108
Phosphate buffer	0.00032	Biotinilation	0.0015
Washing buffer	0.0081	PBS	0.0003
Secondary Ab	0.021	QD	0.030
Substrate	0.0003		
Stop buffer	0.0004		
Total	0.107	Total	0.086

^{a)} Estimation of the cost of the antibody produced by our research team.

Table S5. Technical comparison between indirect ELISA and nanoBV.

INDIRECT ELISA		nanoBV	
Procedure	Time (min)	Procedure	Time (min)
Antigen incubation	120	Sample placement / single-step bioassay	30
Blocking	40	Kinetics monitoring	120
Primary Ab incubation	120		
Secondary Ab incubation	120		
Reveal	20		
Washing	60		
Reading	5		
Total	485		150

Table S6. Evaluation of the precision of nanoBV in terms of CV. Inter-assay evaluation resulting from 7 assays (performed in different microwell plates).

<i>[SLD], (ng mL⁻¹)</i>	<i>Mean</i>	<i>Standard deviation</i>	<i>CV</i>
<i>Blank</i>	0.368	0.027	7.362 %
<i>1.56</i>	0.437	0.034	7.856 %
<i>3.13</i>	0.462	0.037	7.946 %
<i>6.25</i>	0.486	0.037	7.585 %
<i>12.5</i>	0.501	0.037	7.314 %
<i>25</i>	0.517	0.033	6.318 %
<i>50</i>	0.533	0.031	5.820 %
<i>100</i>	0.547	0.033	5.947 %

Table S7. Evaluation of the LOD of nanoBV across different assays.

<i>Assay number</i> <i>(AN)</i>	<i>LOD</i> <i>(ng mL⁻¹)</i>
<i>AN1</i>	0.01263406
<i>AN2</i>	0.04401915
<i>AN3</i>	0.03341438
<i>AN4</i>	0.11202322
<i>AN5</i>	0.03253999
<i>AN6</i>	0.02614811
<i>AN7</i>	0.04977402

Supporting References

- [1] Cortés-Sarabia, K., Rodríguez-Nava, C., Medina-Flores, Y., Mata-Ruiz, O., López-Meza, J. E., Gómez-Cervantes, M. D., Parra-Rojas, I., Illades-Aguiar, B., Flores-Alfaro, E., and Vences-Velázquez, A. (2020) Production and characterization of a monoclonal antibody against the sialidase of *Gardnerella vaginalis* using a synthetic peptide in a MAP8 format, *Appl Microbiol Biotechnol*.